Quasiparticle band structure and optical properties of α-MnO_2: a beyond density functional theory investigation

M. Chepkoech,[1,*] D. P. Joubert,[1] and G. O. Amolo[1,2]

[1]The National Institute for Theoretical Physics, School of Physics and Mandelstam Institute for Theoretical Physics, University of the Witwatersrand, Johannesburg Wits 2050, South Africa

[2]Department of Physics and Space Science, The Technical University of Kenya, P.O. Box 52428-00200, Nairobi, Kenya

E-mail: chepkoechmirriam@gmail.com

Abstract. The quasi-particle band structure and the optical properties of spin polarized bulk α-MnO_2 have been investigated by means of many body perturbation theory within an *ab initio* framework. As a starting point the electronic band structure obtained from Density Functional Theory with a Hubbard correction (DFT+U, U = 2.4 eV) shows that bulk α-MnO_2 is a semiconductor with a band gap of 1.284 eV. The quasiparticle band structure at the $scGW_0$ many body perturbation level of approximation yields a fundamental band gap of 2.20 eV. Moreover, for the optical properties calculations, two particle excitations have been included through solving the Bethe-Salpeter equations (BSE). From our results, the α-MnO_2 exhibits strong optical absorption in the visible region along all the crystallographic directions. The optical anisotropy in this material is analyzed by means of the dielectric function as well as the optical absorption coefficients along different principal axes. The optical absorption spectrum predicts strongly bound excitons that lie below the calculated quasiparticle band gap with binding energy of 0.60, 0.40 and 0.07 eV in bulk α-MnO_2.

1. Introduction

The demand for clean and sustainable energy has emerged to be a driving force in the search of alternative energy sources and efficient storage devices. To mitigate this energy crisis, solar cell technology has attracted great attention promising to replace the fossil-fuel based energy production. This can be realized through the use of lightweight, environmentally friendly and relatively cheap materials in the development of the solar cells. Manganese dioxide (MnO_2) is a transition metal oxide semiconductor which exhibits unique chemical and physical properties due to its complex and flexible crystal structure and morphology. MnO_2 has numerous applications ranging from catalysts, ion sieves in industries, electrode material for rechargeable batteries to energy storage devices [1-4]. It has also attracted considerable attention in many areas of research such as portable electronics, optoelectronics, photovoltaic cells and supercapacitors due to its relative abundance, low toxicity, low cost as well as unique power and energy densities. It exists in various polymorphs namely α, β, γ, λ and differ from one another in the way the MnO_6 octahedral units are packed. Their band gaps fall in the infra red and visible regions of the absorption spectrum and are therefore potential candidates for solar cell applications.

The excited electronic states properties of semiconductors are of great importance since they play a crucial role in physical properties such as electrical conductivities and optical absorption. Computational design of the solar energy materials requires accurate description of the ground-state and excited-state properties. It is known that density functional method [5] provide accurate ground state properties but fails to describe the excited state properties of materials [6]. Thus the main aim of this work is to investigate the quasiparticle band structure and optical properties of bulk α-MnO_2 using first principles calculations and many-body Green's function perturbation theory methods. The electronic and the magnetic properties of this compound have been studied extensively [7]. However, we are not aware of any experimental or theoretical studies of excited states properties of bulk α-MnO_2. Experimental work has studied the structural and optical properties of 1-dimensional α-MnO_2 nanowires and β-MnO_2 nanofibres [8]. This paper is organized as follows. In Section 2, we briefly describe the computational techniques adopted in this work. In Section 3, we present the results and discussions of the structural, electronic and optical properties of α-MnO_2. Finally, a summary and conclusion is provided in Section 4.

2. Computational methods

Density Functional Theory (DFT) and post-DFT many-body perturbation theory techniques as implemented in Vienna *ab initio* Simulation Package (VASP) [9-14] was used to investigate the electronic and optical properties of bulk α-MnO_2. In this implementation a Projector Augumented Wave method [11, 15] to describe the interactions between the core and the valence electrons. The Generalized Gradient exchange correlation approximation (GGA) in the form of Perdew, Burke and Ernzerhof [16] with a Hubbard correction (PBE+U) [17-19] was employed. The PBE+U approximation has been demonstrated to give a good description of electronic properties of manganese oxides. PBE+U calculations were carried out following the version of Dudarev *et al.* approach [20] as implemented in the VASP code [17-19]. We applied the U on the 3d states of Mn atoms. We used several U values until we obtained band gap values that were in good agreement with the experimental values. A Hubbard parameter U = 2.4 eV was adopted in this study. The GW type of pseudopotentials supplied through VASP (v.52) were adopted in our calculations. A plane wave basis set with kinetic energy cut-off of 300 eV was employed. Brillouin zone integration was performed using an 8×8×2 k-point grid centered on Γ to ensure convergence of the Kohn-Sham eigenvalues. Starting from the (PBE+U) eigenfunctions and eigenenergies, we calculated the quasiparticle energy correction by adopting the partially self consistent $scGW_0$ level of approximation [21, 22]. In this approximation the wavefunctions and the quasi-particle energies are updated while the screened Coulomb interaction is kept at the DFT level of approximation. Four cycles were needed for convergence. To study the excitonic effects, optical properties were investigated within the BSE level of approximation. All the BSE calculations were performed by employing the Tamm-Dancoff approximation [23-25]. In order to converge the optical excitations that lie in the low frequency regime, we considered the 24 highest valence bands and 24 lowest conduction bands.

3. Results and discussions

3.1. Structural properties

α-MnO_2 crystallizes in a body centered tetragonal structure belonging to the 14/m space group (No. 87). It consists of double chains of MnO_6 which forms 2×2 tunnels along the c axis. Experimentally [26], it is known to posses antiferromagnetic ordering at low temperatures. The antiferomagnetic ordering displayed in Figure 1(a) have been used throughout our entire calculations. The primitive and the conventional unit cells of α-MnO_2 are shown in Figure 1(a) and (b). We present the calculated cohesive energies and primitive cell volumes fitted to the third-order Birch Murnaghan Equation of State in Figure 1(c). For each volume the atoms were allowed to relax till the forces were less than 5 meV/$\mathring{A}$. The calculated structural properties,

i.e., the lattice constants a and c, unit-cell volume Ω, cohesive energy E_{coh} and Bulk modulus B of α-MnO_2 are summarized in Table 1 together with other theoretical and experimental data. Our computed lattice parameters are in good agreement with the experimental values.

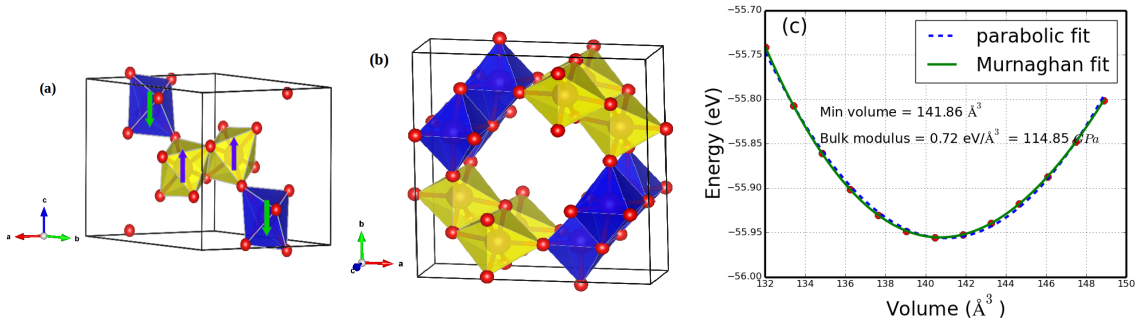

Figure 1. (a) Primitive unit cell showing spin orientations of the Mn atoms in the oxygen octahedra. The green arrows show Mn atoms with spin down magnetic moments whereas the purple arrows show Mn with spin up magnetic moments. (b) Conventional unit cell of α-MnO_2. (c) calculated cohesive energies vs. primitive cell volumes for α-MnO_2

Table 1. Experimental data and calculated structural parameters for α-MnO_2.

Structural parameters	$a(\AA)$	$c(\AA)$	$\Omega(\AA^3)$	E_{coh}(eV/atom)	B(GPa)	
PBE+U (U = 2.4)	9.869	2.913	283.83	-4.42	114.85	This work
Expt.[27]	9.750	2.861	271.97	-	-	
Expt.[28]	9.784	2.863	274.07	-	-	
Ref.[29]	9.887	2.920	285.03	-	-	

3.2. Quasiparticle spectrum

The quasiparticle band structure of α-MnO_2 was studied by using many body perturbation theory. The Brillouin zone of the body centered tetragonal crystal of α-MnO_2 is shown in Figure 2 [Left]. The band structure of α-MnO_2 calculated from DFT+U and scGW$_0$ approximations along high symmetric directions in the Brillouin zone is presented in Figure 2 [Middle]. The top of the valence band has been shifted to zero for both calculations. The scGW$_0$ band structure displays an indirect band gap with the valence band maxima located at M and the conduction band minima located at X which is in agreement with our PBE+U results and those obtained by Ref. [28] that found an indirect band gap of 1.40 eV using PBE+U. Our predicted band gap value for α-MnO_2 using PBE+U was found to be 1.284 eV which is in excellent agreement with the experimental measured value, E_g = 1.32 eV [30]. The scGW$_0$ calculations shift the band gap from 1.284 eV to 2.20 eV as expected [31]. In order to understand the nature of the electronic band structures, the density of states of α-MnO_2 and the projected density of states of Mn and O elements calculated by scGW$_0$ are displayed in Figure 2 [Right]. It is observed that the valence bands are mainly occupied by the O 2p states with a mixture of Mn 3d states, while the conduction bands are dominated by Mn 3d states with a mixture of O 2p states. This mixture implies presence of hybridization between Mn 3d and O 2p states.

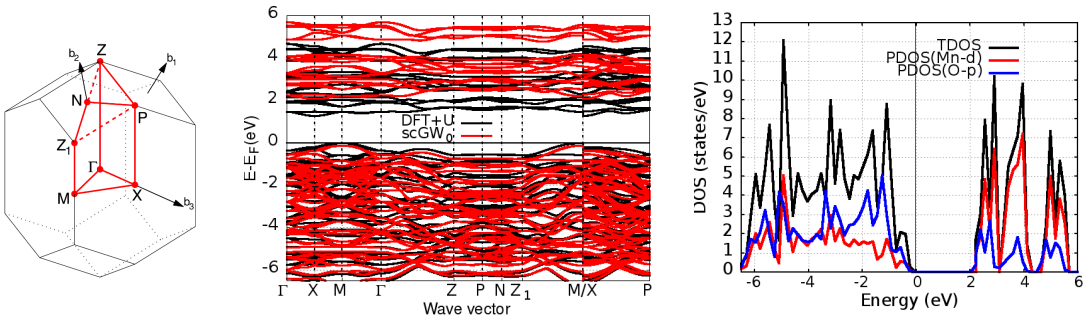

Figure 2. [Left]Brillouin zone of the body centered tetragonal crystal of α-MnO_2, [Middle] band structure calculated using DFT+U (black solid lines) and $scGW_0$ (red solid lines) and [Right] total and projected density of states using the $scGW_0$ approximation.

3.3. Optical properties

To obtain the optical excitons which are not given by the GW level of approximation, BSE calculations were done on top of the partially self consistent $scGW_0$ approximation. Optical properties of α-MnO_2 were investigated by means of a complex dielectric function $\varepsilon(\omega)$ which is expressed as $\varepsilon_1(\omega)+i\varepsilon_2(\omega)$ where $\varepsilon_1(\omega)$ and $\varepsilon_2(\omega)$ are the real and the imaginary parts of the dielectric function. Since α-MnO_2 has a tetragonal symmetry, we have evaluated the dielectric function for two independent principle components i.e. $\varepsilon_a(\omega)$ and $\varepsilon_c(\omega)$ which correspond to light polarized parallel and perpendicular to the c axis. Due to the symmetry, we have compared our optical related constants in two directions. The imaginary and the real parts of the dielectric function as a function of the photon energy along a and c directions are depicted in Figure 3(a) and (b). The imaginary part of the dielectric function, $\varepsilon_2(\omega)$ shows various peaks at different photon energies i.e. the main peaks occurs between energy values 2.5-3.4 eV, which correspond to interband transitions from the valence bands to the conduction bands. The prominent peaks in $\varepsilon_1(\omega)$ are situated at 2.25(2.54) eV along $a(c)$ directions, which are located at the visible range of the spectrum. The static real part of the dielectric function $\varepsilon(0)$ along $a(c)$ axes are 6.56(8.81) respectively. Unfortunately, experimental data are unavailable for comparison.

Related constants such as absorption coefficients $\alpha(\omega)$, optical reflectivity $R(\omega)$, refractive index $n(\omega)$ and energy loss $L(\omega)$ were determined from the values of $\varepsilon(\omega)$. The absorption coefficient as a function of photon energy is presented in Figure 3(c). From the $\alpha(\omega)$ spectrum, the

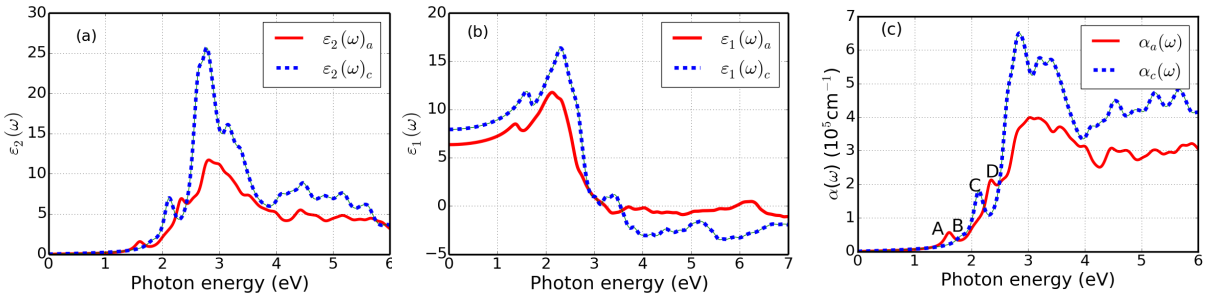

Figure 3. (a) Imaginary part of the dielectric function $\varepsilon_2(\omega)$, (b) real part of the dielectric function $\varepsilon_1(\omega)$ and (c) optical absorption spectrum $\alpha(\omega)$ of α-MnO_2 as a function of photon energy within the BSE level of approximation.

highest absorption peaks are situated in the visible region and are consistent with the interband transitions between the high symmetric k-points in the electronic band structure. For instance,

the first peak corresponds to the transition from the valence band maximum located at M to the conduction band minimum located at the X point. Additionally, it is observed that the main peaks in $\alpha_c(\omega)$ are higher than those in $\alpha_a(\omega)$ which clearly show that the absorption is greater in the c axis than in the a axis. It should be noted that this compound may be a good absorber in the visible region. It is noted that the lowest absorption band edge at $a(c)$ axes respectively occurs at 1.35(1.56) eV which clearly show a difference of 0.21 eV. This significant difference in the absorption edge implies that α-MnO_2 exhibits anisotropic behaviour. Thus the estimated optical band gap for α-MnO_2 was found to be $\sim$1.35 eV which is in agreement with the experimental measured value. In the low frequency regime, the optical absorption spectrum predicts bound excitons that lie below the quasiparticle band gap. The approximate binding energies of excitons are determined by finding the difference in energy between the quasiparticle band gap and the peaks of the BSE absorption spectrum. We estimated the energies of the excitons in the low lying frequency regions of the absorption spectrum and compared with the calculated quasiparticle band gap. The binding energies of the excitons are presented in Table 2. Positive and negative values of binding energies implies the presence of bound and resonant excitons respectively at a given energy. Figure 4(a) shows a refractive index of α-MnO_2.

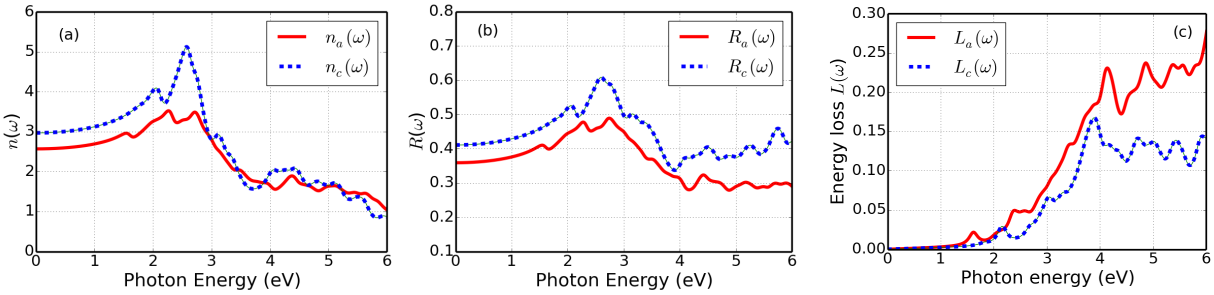

Figure 4. Calculated (a) refractive index $n(\omega)$, (b) optical reflectivity $R(\omega)$ and (c) energy loss L(ω) spectrum of α-MnO_2 as a function of photon energy.

Table 2. BSE calculated positions of A, B, C and D peaks and the corresponding binding energies of excitons in eV for α-MnO_2.

Peaks	E^A	E^B	E^C	E^D
	1.60	1.80	2.13	2.34
Binding energies	0.60	0.40	0.07	-0.14

At first glance, one may notice a similarity between the line shape of $n(\omega)$ and that of $\varepsilon_1(\omega)$ which is due to $n(\omega) = \sqrt{\varepsilon_r}$ relation. We also noticed considerable anisotropic behaviour throughout the spectra. It is also clear that the refractive index of this compound is high in the optical region i.e 1.65 eV - 3.1 eV and gradually decreases beyond this point. The static refractive index $n(0)$ along the $a(c)$ directions were found to be 2.56(2.97) respectively and shows that the light polarized along a is less refracted than along the c direction. The calculated optical reflectivity $R(\omega)$ as a function of photon energy is illustrated in Figure 4(b). We obtained a maximum value of reflectivity of around 61(49)% respectively along the $a(c)$ axes and occurs at the visible region. The energy loss function $L(\omega)$ spectra is presented in Figure 4(c). This quantity describes theoretical energy loss of a fast electron transversing in a material. The peaks in the $L(\omega)$ spectra displays characteristics features associated with the plasma resonance [32]

and the corresponding frequencies are referred to as plasma frequencies. The $L(\omega)$ spectra peaks shows trailing edges in the reflection spectra.

4. Conclusion

In conclusion, the electronic properties of α-MnO_2 were investigated using spin polarized Density Functional Theory with a Hubbard correction U. We obtained a DFT+U band gap of 1.284 eV which is in good agreement with the experimental values whereas the calculated quasi-particle fundamental band gap is 2.20 eV and occurs between the M→X high symmetry directions. We also studied the optical properties of α-MnO_2 where we included the electron-hole interaction on top of partially self consistent $scGW_0$ through solving the Bethe-Salpeter equations which produced an optical band gap of 1.35 eV which is in excellent agreement with the experimentally observed one, $E_g = 1.32$ eV [30]. We observed that the optical absorption spectra exhibit anisotropic behaviour which strongly depends on the polarization direction of the incident light. It was noted that α-MnO_2 absorbs violet light as evidenced by the main peak in the absorption spectrum. Moreover, optical absorption spectra predicts the existence of bound excitons in the low lying frequency regions.

Acknowledgments

We wish to acknowledge the financial support from AIMS-DAAD. We are also grateful to the Centre for High Performing Computing, South Africa, for providing us with the computational facilities.

References

[1] Kumar R, Sithambaram S and Suib S 2009 *J. Catal.* **262** 304
[2] Wang L, Meng C, Han M and Ma W 2008 *J. Colloid Interface Sci.* **325** 31
[3] Thackeray M M 1997 *Prog. Solid State Chem.* **25** 1-71
[4] Cheng F, Zhao J, Song W, Li C, Ma H, Chen J and Shen P 2006 *Inorg. Chem.* **45** 2038
[5] Hohenberg P and Kohn W 1965 *Phys. Rev.* **140** 1133
[6] Aulbur W, Jönsson L. and Wilkins J 1999 *Solid State Physics* **54** 1-218
[7] Franchini C, Podloucky R, Paier J, Marsman M and Kresse G 2007 *Phys. Rev.* B **75** 195128
[8] Rajamanickam N, Ganesan P, Rajashabala S and Ramachandran K 2014 *AIP Conf. Proc.* **1591** 267-269
[9] Kresse G and Hafner J 1993 *Phys. Rev.* B **47** 558
[10] Kresse G and Furthmuller J 1996 *Comput. Mater. Sci.* **6** 15
[11] Kresse G and Joubert D 1999 *Phys. Rev.* B **59** 1758
[12] Furthmuller J, Cappellini G, Weissker H C and Bechstedt F 2002 *Phys. Rev.* B **66** 155208
[13] Shishkin M and Kresse G 2006 *Phys. Rev.* B **74** 035101
[14] Shishkin M and Kresse G 2007 *Phys Rev.* B **75** 235102
[15] Blochl P E 1994 *Phys. Rev.* B **50** 17953
[16] Perdew J P, Burke K and Ernzerhof M 1996 *Phys. Rev. Lett.* **77** 3865
[17] da Silva J L F, Ganduglia-Pirovano V, Sauer J, Bayer V and Kresse G 2007 *Phys. Rev.* B **75** 045121
[18] Franchini C, Bayer V, Podloucky R, Paier J and Kresse G 2005 *Phys. Rev.* B **72** 045132
[19] Franchini C, Podloucky R, Paier J, Marsman M and Kresse G 2007 *Phys. Rev.* B **75** 195128
[20] Dudarev S L, Botton G A, Savrasov S Y, Humphreys C J and Sutton A P 1998 *Phys. Rev.* B **57** 1505
[21] Hedin L 1965 *Phys. Rev.* **136** A796
[22] Hedin L and Lundqvist S 1970 *Solid state Phys.* **23** 1-181
[23] Salpeter E and Bethe H A 2001 *Phys. Rev.* **86** 6
[24] Albrecht S, Reining L, Del Sole R and Onida G 1998 *Phys. Rev. Lett.* **80** 4510
[25] Rohlfing M and Louie S G 1998 *Phys. Rev. Lett.* **81** 2312
[26] Yamamoto N, Endo T, Shimada M and Takada T 1974 *Jpn. J. Appl. Phys.* **13** 723
[27] Yang J B, Zhou X D, James W J, Malik S K and Wang C S 2004 *Appl. Phys. Lett.* **85** 3160
[28] Fritsch S, Post J E, Suib S L and Navrotsky A 1998 *Chem. Mater.* **10** 474
[29] Yusuke N, Kaoru O and Shinichiro N 2016 *Phys. Chem. Chem. Phys.* **18** 13294-13303
[30] Gao T, Fjellvag H and Norby P 2009 *Anal. Chim. Acta* **648** 235
[31] Kobayashi S, Nohara Y, Yamamoto S and Fujiwara T 2008 *Phys. Rev.* B **78** 155112
[32] Fox M 1972 *Optical Properties of Solids*, Academic Press, New York